Multiple scattering of acoustic waves with application to the index of refraction of fourth sound

David Linton Johnson and Pabitra N. Sen
Schlumberger-Doll Research Center, P. O. Box 307, Ridgefield, Connecticut 06877
(Received 12 Janary 1981)

A multiple-scattering model which previously explained the conducting properties of fluid-saturated porous fused glass beads is applied to the acoustic index of refraction n of an ideal fluid in a rigid porous frame. The model consists of ellipsoidal grains coated with an effective medium consisting of fluid and other fluid-coated grains; this nesting is continued *ad infinitum* in order to insure connectedness of the pore space to very low values of porosity. For the relevant cases considered here, the result is $n^2 = P^{-\beta}$, where P is the porosity and β depends on the aspect ratio of the grains. By assuming that the scatterers used in fourth-sound experiments can be characterized by long filaments or needles, randomly oriented ($\beta = \frac{2}{3}$), we have achieved excellent agreement with experimental values of n^2; the data also seem to agree with an earlier theory valid for low concentration of aligned needles ($n^2 = 2 - P$), when extrapolated to high concentrations of scatterers ($\gtrsim 50\%$). The present theory contains neither approximation. We also resolve a controversy over the relationship between n and the hydrodynamic drag parameter λ; the correct result is $n^2 = (1-\lambda)^{-1}$.

I. INTRODUCTION

The scattering of waves or the flow of electrical current around obstacles which have well-defined simple geometries and which have known moduli, densities, conductivities, etc. are examples of a class of problems which appears in many textbooks dating back over one hundred years.[1] If there is a finite concentration of such obstacles (approaching or even exceeding 50%) there is interaction between the obstacles due to multiple scattering of the wave or current density off one object before it encounters another. Such problems are exacerbated if the geometry of the scattering centers is not easily characterized. Some simplification occurs if the scattering objects are inert—the electrical conductivity of a nonconducting matrix filled with a conducting pore fluid, or acoustic-wave propagation through an ideal (nonviscous, nonthermally conducting) fluid occupying the pore space of a rigid skeletal frame. Realizable examples of the former can easily be found, examples of the latter can be approximated by gases in a solid matrix although thermal and viscous effects are generally quite appreciable. One example of the latter which is realizable to a high degree of accuracy is fourth sound[2] in a superleak system saturated with superfluid ^{4}He, and we shall focus our attention on it in this article.

Fourth sound occurs when ^{4}He below T_λ saturates a superleak material whose pores are so small that the viscosity of the normal component immobilizes it relative to the presumably rigid superleak and only the superfluid component can oscillate. (The moduli of most solids are three orders of magnitude larger than that of helium.) From the two fluid equations of motion in which the velocity of the normal component has been set equal to zero, one can calculate[2] the theoretical speed of fourth sound as a function of temperature, $C_4^0(T)$. This result would apply only for the case of a superleak consisting of a parallel collection of narrow straight capillary tubes. The porous superleak materials actually used in practice[2] have a tortuous, branching pore space, and the renormalized experimental speed of fourth sound, $C_4^E(T)$ = (sample length)/(arrival time), is less than the theoretical value. The ratio of the two is defined to be the index of refraction, n, which is a geometrical factor presumed to be temperature independent:

$$C_4^E(T) = \frac{C_4^0(T)}{n} \quad . \tag{1.1}$$

Obviously $n = 1$ for a straight tube because the speed of sound in a fluid confined by a rigid straight tube is the same as that for an unbounded medium, but $n > 1$ for a packed powder sample, reflecting the multiple scattering of the wave by the obstacle course. Currently, there is no satisfactory first-principles theory of n and it is the purpose of this article to provide some progress in that direction.

From the multiple scattering point of view, the theory of the renormalization of the fourth-sound velocity is equivalent to solving for the motion of an ideal, nonviscous fluid, subject to the boundary condition that the perpendicular component of fluid velocity must vanish at the fluid-matrix interface. In Sec. II we elaborate on the connection between the

acoustic index of refraction and the electrical conductivity of the nonconducting superleak saturated with a conducting fluid. In Sec. III we use this analysis to resolve in a simple manner a controversy involving the relationship between n and the hydrodynamic drag parameter. In Sec. IV we use an existing theory of electrical conductivity in disordered systems to calculate the index and compare with existing experimental data on systems having air or superfluid ^{4}He as the pore fluid. Salient features of our results are emphasized in Sec. V. We are, of course, not concerned in this article with superleaks whose pores are so small that size effects modify the superfluid.

II. RELATION BETWEEN THE ACOUSTIC INDEX OF REFRACTION AND ELECTRICAL CONDUCTIVITY

The concept of an index of refraction has meaning only if the wavelength is much larger than any characteristic pore or grain size; on a microscopic scale one is always in the near zone and the microscopic flow pattern is then the same as that of the steady flow of an incompressible fluid[3] times $\exp(-i\omega t)$, where ω is the frequency. Therefore, the index of refraction, n, is independent of the fluid characteristics (density or modulus) and is purely a geometrical quantity. In this section we wish to explore the connection between this parameter and the dc electrical conductivity of the pore space.

Consider, then, an ideal nonviscous, thermally nonconducting fluid of density ρ_f and adiabatic bulk modulus K (its speed of sound is then $V_f=\sqrt{K/\rho_f}$), and imagine that it saturates the pores of a solid matrix whose porosity is P. Imagine that the matrix material is so much stiffer than the fluid that it is immobile. Assume also that any relevant time τ and length d characteristic of the times and distances over which the fluid motion undergoes significant changes satisfy the inequality

$$\tau \gg d/V_f \ .$$

This requirement of low frequency guarantees that "the fluid may be regarded as incompressible" as far as the *microscopic* flow pattern of the fluid is concerned.[4]

Consider a surface element of area dA in the porous fluid-filled system. Part of this surface cuts through solid and only PdA is in contact with the fluid. (For statistically homogeneous, isotropic pore structures the two-dimensional porosity on a surface cut is equal to the three-dimensional volume porosity.) Therefore, the total force on the fluid that is in contact with the surface element is $P\mathcal{P}dA$ where $\mathcal{P}$ is the fluid pressure. Similarly, the net force on all the fluid inside a volume dV_0 is

$$\vec{\mathcal{F}}=-P\vec{\nabla}\mathcal{P}dV_0 \ . \tag{2.1}$$

The effective density, ρ^*, is defined so that the acceleration $d\vec{v}/dt$, of the fluid inside dV_0, is related to Eq. (2.1), for a nonviscous fluid:

$$\rho^* P\frac{d\vec{v}}{dt}dV_0=-P\vec{\nabla}\mathcal{P}dV_0 \ . \tag{2.2}$$

Here $\vec{v}$ is the time rate of change of position of the fluid; $P\vec{v}dA$ is the rate at which fluid crosses dA. Obviously, for a collection of straight tubes parallel to the direction of motion, and arbitrary porosity, $\rho^*=\rho_f$ (the bulk fluid density). In general, $\rho^*>\rho_f$ reflecting the "Kelvin inertial drag" whereby the momentum of a fluid flowing around an obstacle is altered. These points are nicely discussed in Landau and Lifshitz.[5] The bulk modulus of the fluid is defined by

$$\vec{\nabla}\mathcal{P}=K\frac{\vec{\nabla}\rho_f}{\rho_f} \ . \tag{2.3}$$

Equation (2.3) is a microscopic equation of state; it also gives the relationship between macroscopically averaged quantities as long as the averages of $\vec{\nabla}\mathcal{P}$ and $\vec{\nabla}\rho_f$ are defined in the same way.

Finally, conservation of fluid mass is expressed as

$$\vec{\nabla}\cdot(\rho_f P\vec{v})+\frac{\partial}{\partial t}(\rho_f P)=0 \ . \tag{2.4}$$

Note that ρ_f, and not ρ^*, appears in Eq. (2.4). Combining Eqs. (2.2)–(2.4) in linearized form, it is straightforward to show that all quantities obey a wave equation with speed:

$$V=(K/\rho^*)^{1/2} \ . \tag{2.5}$$

Equation (2.5) defines the speed of sound of an ideal nonviscous fluid in a rigid porous matrix (e.g., fourth sound). It remains to establish the connection between the effective density, ρ^*, and the true density, ρ_f, in the particular microgeometry. In the remainder of this section, we first establish the connection between ρ^*, ρ_f, and the electrical conductivity of the pore space.

Brown[6] has utilized the fact that the differential equation and boundary condidtions governing the motion of an incompressible fluid in the pore space is identical with that of the electrical conduction of the sample if the pores are filled with a conducting fluid. Brown has shown, in effect, that

$$\rho^*=FP\rho_f \ , \tag{2.6a}$$

where F is the ratio of the electrical conductivity, σ_f, of the pore fluid (not necessarily the same fluid as in the acoustic problem) to the conductivity σ of the sample as a whole,

$$F\equiv\frac{\sigma_f}{\sigma} \ . \tag{2.6b}$$

Equations (2.6) hold only if the matrix material is

nonconducting, and there is no interfacial surface conductivity. A summary of the proof is given in Table I. Equations (2.5)–(2.6) imply that the velocity of the normal mode is

$$V=\left(\frac{K}{FP\rho_f}\right)^{1/2}=\frac{V_f}{\sqrt{FP}} \quad . \tag{2.7}$$

This is the desired result because it relates the acoustic index of refraction to the electrical properties of the system:

$$n^2=FP \quad . \tag{2.8}$$

An alternative and more formal proof, based on exact expressions for n^2 and F derived by Bergman,[7,8] is presented in Appendix A. We should mention that Eq. (2.8) was clearly understood in its full generality by Lord Rayleigh[9] who used it in certain special cases, although he does not appear to have published the general proof. Doubtless, others have realized this equivalence.

We conclude this section with a few comments on the significance of Eq. (2.8):

(1) Equation (2.8) is an exact result which can and should be experimentally tested by, for example, saturating a superleak with a saline solution and measuring its conductivity.

(2) Note that for the special case of a collection of straight tubes parallel to the direction of motion or electric field the conductivity is obviously $\sigma=P\sigma_f$, therefore $F=P^{-1}$ and $n=1$ as previously noted.

(3) The index of refraction is scale invariant because when the pore-wall surface effects are negligible, and (2.6) holds, it is easy to show that σ remains unchanged if the sample is uniformly dilated or contracted by a scale factor. The proof essentially was given by Maxwell[10] and has been generalized by Cohen.[11] Accordingly, the refractive index (2.8) is also similarly scale invariant. (See Sec. IV A.) The usefulness of this result is that F and P can be measured on a sample at room temperature to deduce n^2 at low temperature even though the matrix may have contracted thermally.

(4) In all treatments of fourth sound it is implicitly assumed that the fluid motion is completely decoupled from the solid motion. This is certainly true if the moduli of the skeletal frame are much larger than the modulus of the superfluid, as was explicitly shown in Ref. 12. Equation (2.8) is also particularly useful for cases when the modulus of the fluid is comparable to or exceeds that of the solid and one cannot assume the matrix to be rigidly immobile. In a series of papers, Biot[13] proposed an effective-medium theory whereby the average displacement of both solid and fluid parts are followed separately. One of the parameters, $\alpha \geq 1$, the "structure constant" is a purely geometric parameter independent of material parameters which relates the off-diagonal element of the density matrix to the porosity and the fluid density by $\rho_{12}=(1-\alpha)P\rho_f$. It has been shown[12] that when the fluid is much more compressible than the skeletal frame of the solid, one of the modes predicted by the Biot theory has a speed given by $V=V_f/n$ where $n^2=\alpha$; from this point of view

TABLE I. Equivalence between the problem of the electrical conductivity of a nonconducting rigid, homogeneous, and isotropic porous matrix containing a conducting pore material and that of the hydrodynamics of an ideal fluid moving in the same pore space, in the long-wavelength (incompressible fluid) limit. All quantities have their usual meanings; $\hat{n}_w$ is a unit vector normal to the pore-matrix interface, $\hat{n}$ is a unit vector normal to a flat surface of area A over which the integration is performed. The quantity $\vec{B}$ represents the volume flow rate through an area A and is therefore related to the average fluid velocity by $\vec{B}=\langle\vec{v}\rangle PA$. The quantity F, defined by the last entries, is a scalar for statistically homogeneous, isotropic samples. Inasmuch as the two problems are equivalent, the same value of F applies for the two problems for a given sample, and consequently the last row of the table yields Eqs. (2.2), (2.6a), and (2.6b) of the text. See Brown (Ref. 6) for details.

Elec. Cond.		Hydrodynamics
$\vec{j}=-\sigma_f\nabla\Phi$	Microscopic relation	$\frac{\partial\vec{v}}{\partial t}=-\frac{1}{\rho_f}\vec{\nabla}\mathcal{P}$
$\nabla^2\Phi=0$	Differential equation	$\nabla^2\mathcal{P}=0$
$\vec{j}\cdot\hat{n}_w=0$	Boundary condition	$\vec{v}\cdot\hat{n}_w=0$
$\vec{I}=\int\int(\vec{j}\cdot\hat{n})\,dA\,\hat{n}$	Definition	$\vec{B}=\int\int\vec{v}\cdot\hat{n}\,dA\,\hat{n}$
$\vec{I}=-\frac{A}{F}\sigma_f\langle\nabla\vec{\Phi}\rangle$	Macroscopic solution	$\frac{\partial\vec{B}}{\partial t}=-\frac{A}{F}\frac{1}{\rho_f}\langle\vec{\nabla}\mathcal{P}\rangle$

fourth sound is seen to be a special case of the "Biot slow wave" and consequently values of $\alpha = n^2 = FP$ deduced for one pore fluid (superfluid ^{4}He) can be used for another (e.g., water, mercury) even if the fluid and solid moduli are comparable, or indeed if the fluid is less compressible than the solid. More importantly, a measurement of the electrical conductivity can also be used to deduce α.

In passing we point out that in the opposite limit of an unconsolidated solid matrix, corresponding to vanishing skeletal frame moduli, Eqs. (2.7) and (2.8) are still valid provided that there is a large acoustic impedance mismatch between fluid and solid constituents. These points are discussed in another article.[14]

(5) Although Eq. (2.8) is exact, it applies only to the zero-frequency limit of $n(\omega)$. If there are large isolated pore regions connected by small long necks to the main pore region (Helmholtz resonators) then $n(\omega)$ can have an appreciable frequency dependence even at wavelengths large compared to typical pore sizes; it diverges, in fact, at the resonance frequency.[15]

III. RELATIONSHIP BETWEEN THE ACOUSTIC INDEX OF REFRACTION AND THE COEFFICIENT OF HYDRODYNAMIC DRAG

In this section we make a slight digression and use the results of Sec. II in order to make a simple comment on a relationship involving n^2 which was derived by Revzen *et al.*[16] and which has been claimed to be incorrect by Bergman *et al.*[7] If a superleak is pulled through a He II bath at constant speed v_R then, because the superfluid is forced around the tortuous pore space, it acquires a macroscopic velocity $v_s \leq v_R$ or,

$$v_s = \lambda v_R \ , \tag{3.1}$$

where the hydrodynamic drag parameter, λ, has values between 0 and 1. Note that this effect is *not* dependent on viscous forces which are absent for a superfluid. (The normal component, if there is any, is locked relative to the superleak by its viscosity.) Revzen *et al.*[16] claim the following relationship:

$$n^2 = P/(1-\lambda) \ , \tag{3.2}$$

which was first disputed by Bergman *et al.*[7] who claim

$$n^2 = 1/(1-\lambda) \ . \tag{3.3}$$

That Eq. (3.3) is incorrect can be seen most simply by considering a collection of straight tubes of arbitrary porosity all parallel to the direction of fluid motion for which $n=1$, $\lambda=0$, and $P \neq 1$. The faulty equation is Eq. (4) of Ref. 16 which should read (in our notation)

$$\vec{F}_{\text{ext}} = -\Omega P \vec{\nabla} \Phi \ . \tag{3.4}$$

Here, $\vec{F}_{\text{ext}}$ is the net force due to pressure on the fluid contained within a volume Ω of the sample (the volume of the fluid alone is ΩP). The extra factor of porosity P, not present in Ref. 16, arises from the same reason that leads to the factor of porosity in Eq. (2.1) of the present article. [If it were absent, Eq. (2.8) would read $n^2 = F$ which is obviously wrong as can be seen in comment (2) of Sec. II.] The remainder of the derivation is correct; the drag force that the solid matrix exerts on the superfluid is

$$\vec{F}_d = -\frac{\Omega P \rho_f \lambda}{1-\lambda}\left(\frac{d\vec{v}_s}{dt} - \frac{d\vec{v}_R}{dt}\right) \tag{3.5}$$

and so the equation of motion for the superfluid, when the solid matrix superleak is at rest, is

$$\Omega P \rho_f \frac{d\vec{v}_s}{dt} = -\frac{\Omega P \rho_f \lambda}{1-\lambda}\frac{d\vec{v}_s}{dt} - \Omega P \vec{\nabla} \Phi \ . \tag{3.6}$$

Continuing the derivation of Ref. 16 but using our Eq. (3.4) instead of their Eq. (5) one is led to Eq. (3.3) as claimed, correctly, by Bergman *et al.*[7] Alternatively, Eq. (3.6) is of the form of Eq. (2.2) with $\rho^* = \rho_f/(1-\lambda) (\equiv n^2 \rho_f)$.

There are at least two different ways in which λ can be measured on a given superleak: (a) by measuring the Doppler shifts of fourth-sound speeds in moving superleaks or (b) by measuring persistent superfluid currents in rotating superleaks. Unfortunately, it does not appear to be the case that there are published values for both n and λ on a given superleak. However, for the powdered alumina superleaks used, it is known that the empirical relationship $n^2 = 2 - P$ gives a remarkably accurate fit to the data; see for example, the discussion in Sec. IV B and especially Fig. 1. For the purposes of this section only, we will assume that $n^2 = 2 - P$ gives a reasonably accurate value of n for a superleak of a given porosity.

It is possible to deduce the value of λ for two different superleaks in which Kojima *et al.*[17] have measured Doppler splittings of fourth-sound resonances. Mehl and Zimmerman[18] have measured λ (χ in their notation) in their study of torsional oscillations and persistent current flow experiments. The data are summarized in Table II in which comparison is made between $1/(1-\lambda)$, $P/(1-\lambda)$, and calculated values of $n^2 = 2 - P$. If the values of n^2 are correct (the value for the $P = 0.78$ superleak has been measured[17] and is equal to 1.24) then there are some disagreements with $n^2 = 1/(1-\lambda)$ indicating a possible breakdown of the validity of the concept of the hydrodynamic drag parameter.

TABLE II. A comparison of experimental values of $1/(1-\lambda)$ and $P/(1-\lambda)$ against n^2 which is assumed to be approximately equal to $2-P$. See text for explanation.

Superleak	P	λ	$1/(1-\lambda)$	$2-P$	$P/(1-\lambda)$
Alumina[a]	0.65	0.46	1.85	1.35	1.20
Alumina[a]	0.78	0.34	1.52	1.22	1.18
Resin[b]	0.59	0.32	1.47	1.41	0.87
Alumina[b]	0.82	0.15	1.18	1.18	0.97
Alumina[b]	0.83	0.13	1.15	1.17	0.95

[a] Kojima *et al.*, Ref. 17. [b] Mehl and Zimmerman, Ref. 18.

IV. SELF-SIMILAR MODEL FOR THE ACOUSTIC INDEX OF REFRACTION

In Sec. IV A we summarize the relevant theoretical results for the electrical conductivity (i.e., F) for systems consisting of nonconducting ellipsoidal grains embedded in a conducting medium and, of course, use these results to derive expressions for the acoustic index of refraction due to incompressible ellipsoidal grains. In Sec. IV B, we compare the results with existing acoustical data.

A. Theory

For a dilute concentration of oriented ellipsoidal scatterers, Fricke[19] has derived an expression for the conductivity from which we deduce n [Eq. (2.8)]:

$$n^2=\frac{1-PL_i}{1-L_i} \quad . \tag{4.1}$$

Here L_i is the depolarization factor in the direction of the applied field or motion of fluid, and it can be calculated explicitly for a given grain shape from Eq. (B2) of Appendix B. Special cases of interest to us are spherical grains, for which $L_i=\frac{1}{3}$, which yields the well-known Maxwell[10] result

$$n^2 \text{ (dilute spheres)} = \tfrac{3}{2}-\tfrac{1}{2}P \quad , \tag{4.2}$$

and needles (extremely prolate spheriods) whose axes are perpendicular to the direction of motion, for which $L_i=\frac{1}{2}$, and therefore,

$$n^2 \text{ (dilute needles } \perp) = 2-P \quad . \tag{4.3}$$

These results are exact in the dilute concentration limit ($P\to 1$).

In order to go beyond the dilute limit, Sen, Scala, and Cohen[20] have proposed a "self-similar model" for the dielectric properties of two-phase composite media with the original goal of understanding the dielectric properties of sedimentary rocks. There, the key observation is that the samples have a finite conductivity at extremely low levels of porosity ($<1\%$). That is, the "percolation threshold" occurs at or near zero porosity because the pore space is highly correlated and thus interconnected even at the low porosities. In order to guarantee the interconnectedness of the pore space in the theory, Sen, Scala, and Cohen[20] build up the rock in steps. The model consists of ellipsoidal grains which in turn are coated by other fluid-coated grains. Coating at each level consists of nested coated ellipsoids. The scale invariance of the problem (see Appendix B) allows us to make the sizes arbitrary. The effective-medium approximation, i.e., the coherent-potential approximation (CPA), is used at each step to compute the effective dielectric constant; a finite concentration of grains is obtained by introducing an infinitesimal amount of grains (dilute limit) in an effective medium consisting of the previous mixture, and then integrating to the final concentration. The trick of nested coating keeps the pore space interconnected and improves the local-field corrections for the single-site approximation. There are, of course, competing theories but we do not focus on them in this article.

If the ellipsoidal grains are nonconducting and the pore material is conducting, the self-similar result for the static conductivity can be expressed under fairly general conditions as

$$F=P^{-m} \quad , \tag{4.4}$$

where m depends on the aspect ratio of the grains through the pertinent depolarization factor. [We have elaborated on Eqs. (4.4)–(4.9) and their conditions of validity in Appendix B.] Note that the self-similar result, (4.4) connects smoothly with (4.1) in the dilute limit where both are exact:

$$n^2=\lim_{P\to 1}(PP^{-m})=\frac{1-PL_i}{1-L_i} \quad . \tag{4.5}$$

For spherical grains $L_i=\frac{1}{3}$, $m=+\frac{3}{2}$ and this result, $\sigma_f/\sigma=P^{-3/2}$, agrees[20] to within 0.1% with the experimental electrical conductivity of fused glass-bead samples saturated with saline water over a

porosity range $P=0.03$ to 0.38. This is strong evidence that the self-similar model can successfully span the range from dilute concentration of scatters (where it is exact) to high concentrations or low porosity. For the acoustics problem we have the result from Eq. (2.8) that

$$n^2 \text{ (self-similar, spheres)} = P^{-1/2} \ , \tag{4.6}$$

which connects smoothly with Eq. (4.2), $n^2=\frac{3}{2}-\frac{1}{2}P$, as P tends to 1.

If the grains consist of extremely prolate spheroids (needles) all of whose major axes are perpendicular to the electric field or direction of motion, then $L_i=\frac{1}{2}$ and $m=+2$ which means

$$n^2 \text{ (self-similar, needles } \perp) = P^{-1} \ . \tag{4.7}$$

This result connects smoothly with Eq. (4.3), $n^2=2-P$, as P tends to 1.

In order to apply the self-similar model to a system of randomly oriented spheroids with equal probability of any orientation, there must be an averaging procedure which was carried out by Veinberg[21] and (was applied to rocks by) Mendelson and Cohen[21] and is discussed in our Appendix B. The exponent m of Eq. (4.4) is then given by

$$m=\int \frac{5-3L_s}{3(1-L_s^2)}P(L_s)\,dL_s \ , \tag{4.8}$$

where $P(L_s)$ is the probability distribution of spheroids whose depolarization factor along the symmetry axis is L_s. For spherical grains with $P(L_s)=\delta(L_s-\frac{1}{3})$ we have $m=\frac{3}{2}$ as before. For randomly oriented needles or filaments $P(L_s)=\delta(L_s)$ and this gives $m=\frac{5}{3}$ which implies that the acoustic index of refraction for an array of randomly oriented needles is, within the context of the self-similar model,

$$n^2 \text{ (self-similar, random needles)} = P^{-2/3} \ . \tag{4.9}$$

B. Comparison with experimental data

As mentioned in the Introduction, fourth-sound experiments correspond to the idealization of wave propagation in a nonviscous fluid occupying the pore space of a rigid matrix; indeed, consideration of the more general Biot theory for coupled fluid to solid motion has indicated[12] that the immobility of the matrix is accurate to one part in 10^4. In this subsection we compare the existing index of refraction data for fourth sound with the self-similar model. We conclude with the analysis of data on propagation in the air-filled pores of a lead-shot matrix.

Rudnick[2,22,23] and co-workers have investigated fourth sound in superleak materials that consisted of loose powders primarily of Cr_2O_3 or Al_2O_3, although carbon black and silica were also used. The powders were compacted under pressure to achieve the desired porosities. Their index of refraction data, for porosities in the range 43% to 94%, are presented in Fig. 1; all data correspond to grain sizes from 500 to 10 000 Å so that there are no healing length effects.[23] Because of the extremely high values of porosity, it is clear that the matrix of scattering centers is far from that of a dense random packing of spheres,[24] for which the porosity is only 38%, and the possibility of intraparticle porosity arises. Micrometer-sized particles of γ-alumina (Al_2O_3) used as catalyst supports actually are aggregates of 50–100 Å sized particles and thus have intraparticle pores[25] of the order 20–30 Å. However, Rosenbaum *et al.*[26] have published scanning transmission electron microscope (STEM) pictures of two superleak powders, a 0.05 μm Al_2O_3 powder (Linde B γ-alumina) and a 1.0 μm Al_2O_3 (α-alumina) powder which give the impression of slightly prolate (elongated) spheroids which are fairly closely packed; in neither of these pictures is the resolution good enough (≈ 0.1 μm) to observe any intraparticle porosity, particularly since the powders were coated with a metallic film for the STEM. In order to establish further the pore sizes a liquid-nitrogen desorption isotherm test was performed[27] and this indicated that, for the 0.05 μm alumina, the pores in the range 0–30 Å accounted for about 0.72% of the sample volume with the remaining porosity in pores in the 200–300 Å range, as expected (total porosity is about 69%). The same test on the 1.0 μm alumina indicated no significant porosity in pores less than 1000 Å, as expected. We conclude that the extremely high values of porosity in some of the samples are probably due to the surface contact forces which can hold small particles in very open, bridging configurations; it is known[28] that ordinary sand, ground to 1 μm size particles, has a porosity of 75% when poured loosely into a container. It is also known[28] generally that aggregates of such small particles do not crack under pressure but deform plastically during compaction. We therefore surmise that the loose powders form more or less long filaments of bridging particles, looking something like strings of pearls, and that, as pressure is applied, the individual particles sinter to form continuous smooth filaments. We therefore take as our working hypothesis (below) the assumption that the matrices can be modeled mathematically as random arrays of long filaments or needles.

We prefer, however, to make our theoretical versus experimental comparison in stages. Consider, first, Eq. (4.3), $n^2=2-P$, for the index of refraction. It contains two highly dubious assumptions: that the scatterers are all perpendicular to the direction of motion, and that the dilute limit holds for all relevant concentrations. Nevertheless, the fit to Rudnick's data is quite good even for fairly low porosities, as

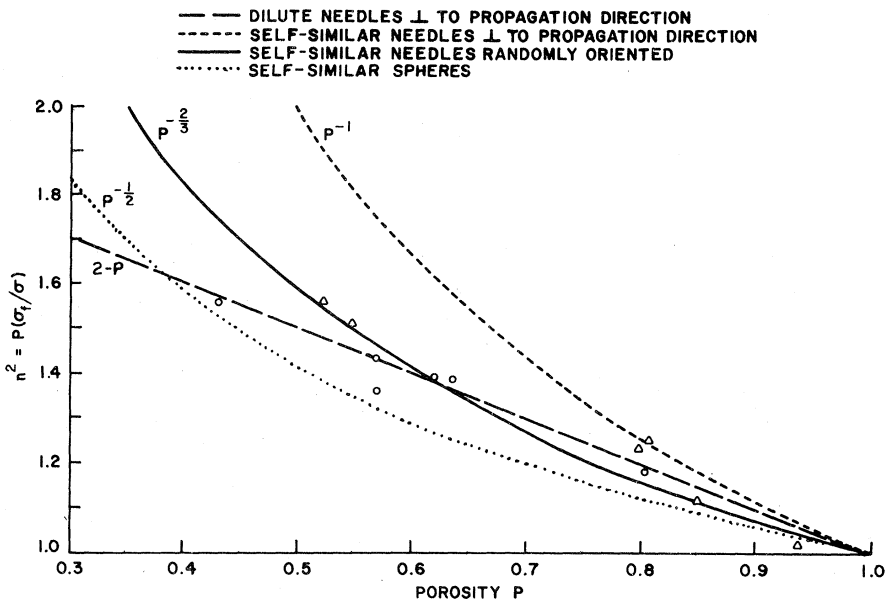

FIG. 1. Acoustical index of refraction n in fourth-sound experiments on packed powder superleaks. The circles are measured values from Ref. 23 and the triangles are measured values from Ref. 22. All curves represent theoretical approximations as explained in the text.

can be seen in Fig. 1 and as originally noted by Rudnick.[22] We wish to eliminate both assumptions.

Second, we consider the self-similar model for needles perpendicular to the direction of propagation, Eq. (4.7), $n^2 = P^{-1}$, which is also plotted in Fig. 1, where it is clear that there is strong diagreement with the data.

Third, the self-similar model for randomly oriented needles, Eq. (4.9), $n^2 = P^{-2/3}$, is plotted in Fig. 1 where it is seen to be in at least as good an agreement with the experimental data as is the empirical expression Eq. (4.3). Unfortunately, the two expressions are nearly identical over the range where the data exists. The most glaring discrepancy between Eq. (4.9) and the data occurs at $P = 43\%$; to achieve this porosity, however, it was necessary to pack the powder with $\sim 10\,000$ psi of pressure which may have severely altered the skeleton shape. We must emphasize that the scattering matrix shapes are not known, however, and we are simply conjecturing, on the basis of the high porosities of these systems, that they consist of a random orientation of needles or filaments each of which may have originally consisted of many individual powder grains. If this conjecture is correct, then the self-similar model agrees quite well with the available experimental data on n and without the two logical difficulties posed by Eq. (4.3) as discussed above. Roughly speaking, the error introduced by the assumption of dilute scatterers and the error introduced by the assumption of oriented scatterers very nearly cancel each other for porosities greater than 50%, although each assumption by itself introduces substantial error.

Finally, we consider the self-similar model for an array of spherical scatterers, $n^2 = P^{-1/2}$, which is also plotted in Fig. 1 and which is, not surprisingly, in strong disagreement with the experimental data. This result represents the lower bound[21] to n^2 within the isotropic self-similar model; it is gratifying that, with one exception, the data all lie above this curve. There is no upper bound; m in Eq. (4.4) can be infinity for extremely oblate spheroids (disks) for which $L_s = 1$. This is because thin flat plates can very effectively block the flow of fluid in the direction perpendicular to the plate.

In connection with the search for fourth sound in ^{3}He, Kojima *et al.*[29] has reported $n^2 = 4.67$ for a 20% porosity superleak of cerium magnesium nitrate (CMN) powder; this is considerably larger than that predicted by the isotropic self-similar model for pro-

TABLE III. Experimental values for the index of refraction of sound propagating in the air-filled pores of a lead-shot matrix; corrections have been made for viscous and thermal effects. Various theroretical predictions are also included for comparison.

P	n^2 Exp.[a]	Self-similar spheres $P^{-1/2}$	Dilute spheres $\frac{1}{2}(3-P)$	Dilute needles, ⊥ $2-P$
0.385	1.64	1.61	1.31	1.62
0.390	1.59	1.60	1.31	1.61

[a] Reference 30.

late spheroids of any eccentricity. Microscopic examination indeed indicates the presence of thin flakes.

We conclude this section with a brief analysis of the much older data of Ferrero and Sacerdote[30] for the speed of sound propagating in the air-filled pores of a matrix of spherical lead shot; the data have been corrected for thermal and viscous effects. Their results are summarized in Table III where it is seen that the self-similar model $n^2=P^{-1/2}$ provides a quite decent fit to the data whereas the dilute spheres or high porosity limit, $n^2=\frac{3}{2}-\frac{1}{2}P$ does not. This is not surprising since the validity of the self-similar model for spherical beads was already established for the electrical case over a much wider and inclusive porosity range. It is accidental that Eq. (4.3) also agrees with the data; the equations $n^2=2-P$ and $n^2=P^{-1/2}$ intersect at $P=0.382$ but differ greatly at other porosities as can be seen in Fig. 1.

V. SUMMARY

We emphasize here the following aspects of this paper.

(1) The problem of the index of refraction of fourth sound can be mapped onto the problem of the electrical conductivity of the pore space. Even if the pore fluid is not superfluid helium, one of the parameters of the Biot theroy, α, is also related to the electrical conductivity. This equivalence, as quantified by Eq. (2.8), ought to be subjected to an experimental verification. The equivalence could fail for fourth sound due to finite-size effects that occur when the pores are small compared to the correlation length. From the electrical side it could fail if there is an appreciable surface conductivity at the fluid-solid interface. In systems for which Eq. (2.8) holds, one can now use the results from the large body of literature on the conductivity of inhomogeneous systems, as we have done in this article. One also has the useful result that $n^2=\alpha=FP$ is scale invariant when interfacial effects are negligible.

(2) The aspect ratio(s) and orientation(s) of the grains are extremely important especially at low porosities (high concentration of grains) as can be seen by comparing or contrasting Eqs. (4.6), (4.7), and (4.9) which are plotted in Fig. 1.

(3) It is also important to go beyond the results for the dilute concentration of scatterers (high porosity); compare Eqs. (4.6) and (4.2) and especially (4.7) and (4.3) which are plotted in Fig. 1. The self-similar model [Eq. (4.6)] has previously been shown to work extremely well in his regard for the case of the electrical conductivity of fused spherical glass bead samples, at very low porosities, whereas the dilute limit, (4.2), fails utterly.

(4) As regards aspect ratios, it would be extremely helpful if scanning electron micrographs of the actual superleak were published so that one could know what to calculate. One might hope to actually measure the statistical distribution of depolarization factors $P(L_s)$ by scanning of serial sections taken from rigid superleaks.

(5) For the superleaks used by Rudnick, one could easily discern between the predictions of the self-similar model for an array of randomly oriented needles, $n^2=P^{-2/3}$, and the result for a dilute concentration of needles perpendicular to the direction of propagation, $n^2=2-P$, simply by going to porosities of 30% or less. Of course, it is important to monitor the shape and orientations of the grains as this is being done.

ACKNOWLEDGMENTS

We are most grateful for extensive conversations with M. H. Cohen, I. Rudnick, and T. J. Plona. We thank R. Kleinberg for providing us with the desorption isotherm data. We are especially grateful to T. J. Plona for spending considerable time with us on the expository nature of the article.

APPENDIX A: FORMAL DERIVATION OF THE EQUIVALENCE OF THE ELECTRICAL CONDUCTIVITY AND THE ACOUSTIC INDEX OF REFRACTION

The formal equivalence of the potential flow in an ideal liquid and the potential problem of electrical properties of inhomogeneous media is useful. There is a vast literature on properties of inhomogeneous material which can be brought to bear onto the problem of fluid flow using this formal analogy.

There are several *equivalent* ways of defining the effective complex dielectric constant ϵ_{eff} for an inhomogeneous medium. The most economic for the present purposes is Eq. (2.9) of Ref. 8, which gives

$$\frac{1}{\epsilon_{\text{eff}}}=\frac{1}{V}\int \epsilon(\vec{r})\,|\vec{\nabla}\phi|^2\,d^3r\Big/\left|\frac{1}{V}\int \epsilon(\vec{r})\nabla\phi\,d^3r\right|^2 . \tag{A1}$$

In (A1) ϕ is the electrostatic potential. For a brine saturated porous matrix made of nonconducting solid, Eq. (A1) gives for the dc conductivity σ, of the rock,

$$\frac{1}{\sigma}=\frac{V}{\sigma_f}\int \theta(\vec{r})\,|\vec{\nabla}\phi|^2\,d^3r\Big/\left|\int \theta(r)(\vec{\nabla}\phi)\,d^3r\right|^2 . \tag{A2}$$

Here $\theta(\vec{r})$ is a function which is unity in the pore space and zero in the insulating solid and σ_f is the conductivity of the fluid. We have used $\epsilon(\vec{r})=1+4\pi i\sigma(\vec{r})/\omega$ and taken the limit $\omega\to 0$. Using the definition of porosity

$$P=\frac{1}{V}\int \theta(\vec{r})\,d^3r\ , \tag{A3}$$

and formation factor

$$F=\sigma_f/\sigma \ , \tag{A4}$$

we find from (A1)–(A4)

$$\frac{1}{FP}=\left|\int \theta(\vec{r})(\vec{\nabla}\phi)\,d^3r\right|^2 \times\left|\int \theta(\vec{r})|\vec{\nabla}\phi|^2\,d^3r\int\theta(\vec{r})\,d^3r\right|^{-1} \ . \tag{A5}$$

This equation is identical to an expression for n^{-2}, the index of refraction of fourth sound given by Eq. (A10) of Bergman, Hohenberg, and Halperin[7] (BHH); the boundary value problem defined by Eqs. (A2) and (A3) of BHH is identical to that defined by Eqs. (4)–(12) of Bergman.[8] The velocity potential ϕ of He is equal to the electrostatic potential apart from a multiplicative constant, which cancels out in (A5) anyway.

Using (A5) and Eqs. (14) and (A10) of BHH we find

$$n^2=FP \ , \tag{A6}$$

which is Eq. (2.8) in the text.

APPENDIX B: THE DEPOLARIZATION FACTORS L AND THE EXPONENT, m, OF THE SELF-SIMILAR MODEL

In this appendix we give explicit formulas for the depolarization factors L_i, L_s in terms of particle shapes and we give the relationship to m of Eq. (4.4).

Consider an ellipsoid of conductivity σ_1, embedded in a medium of conductivity, σ_2, and subjected to an external field $\vec{E}_0$. The field $\vec{E}_0$ can be decomposed into components E_{0x}, E_{0y}, E_{0z} along the axes of ellipsoids. It is easy to show (following, for example, Landau and Lifshitz,[31] pp. 20–27) that the field inside the elliposid is given by

$$E_i=\frac{\sigma_2 E_{0i}}{\sigma_2+(\sigma_1-\sigma_2)L_i} \quad (i=x,y,z) \ , \tag{B1}$$

where L_i is a pure number, given by the integral

$$L_i=\tfrac{1}{2}a_x a_y a_z\int_0^\infty ds\,(s+a_i^2)^{-1} \times[(s+a_x^2)(s+a_y^2)(s+a_z^2)]^{-1/2} \ . \tag{B2}$$

Here a_x, a_y, and a_z are the axes of the ellipsoid; obviously L_i is invariant with respect to uniform expansion or contraction of the ellipsoid. It follows from (B2) that

$$L_x<L_y<L_z \ \text{ if } a_x>a_y>a_z \ , \tag{B3}$$

and

$$L_x+L_y+L_z=1 \ . \tag{B4}$$

For a sphere $a_x=a_y=a_z$, (B2) gives

$$L_x=L_y=L_z=\tfrac{1}{3} \ . \tag{B5}$$

For a circular cylinder with its axis in the x direction ($a_x\to\infty, a_y=a_z$)

$$L_x=0, \quad L_y=L_z=\tfrac{1}{2} \ . \tag{B6}$$

For a plate, with its face perpendicular to the x direction ($a_y, a_z\to\infty$)

$$L_x=1, \quad L_y=L_z=0 \ . \tag{B7}$$

The elliptic integral (B1) can be expressed in terms of elementatry functions for the special case of spheroids, ($a_y=a_z$). For a prolate spheroid ($a_x>a_y=a_z$) of eccentricity $e=(1-a_y^2/a_x^2)^{1/2}$ the depolarization ratio L_s along the symmetry axis (the x axis) is

$$L_s=L_x=\frac{1-e^2}{2e^3}\left(\ln\frac{1+e}{1-e}-2e\right) \ ; \tag{B8}$$

$$L_y=L_z=\tfrac{1}{2}(1-L_s) \ .$$

For an oblate spheroid ($a_x<a_y=a_z$), $e=(a_y^2/a_x^2-1)^{1/2}$

$$L_s=L_x=\frac{1+e^2}{e^3}(e-\tan^{-1}e) \ ; \tag{B9}$$

$$L_y=L_z=\tfrac{1}{2}(1-L_s) \ .$$

(Note that we continue to denote the x axis as the symmetry axis for all spheroids whereas several texts[31,32] have chosen the x axis as the symmetry axis for prolate spheroids but the z axis as the symmetry axis for oblate spheroids.)

For the nearly spherical cases, $e\ll 1$, (B8) and (B9) give

$$\begin{aligned} L_s&=\tfrac{1}{3}-\tfrac{2}{15}e^2 \ \text{(prolate)} \ , \\ L_s&=\tfrac{1}{3}+\tfrac{2}{15}e^2 \ \text{(oblate)} \ . \end{aligned} \tag{B10}$$

We now discuss the relationship between m in Eq. (4.4) and (L_i) for an arbitrary concentration of scatterers as given by the self-similar model[20] for insulating grains ($\sigma_1=0$) embedded in a conducting host fluid ($\sigma_2=\sigma_f$). In general both the conductivity of the sample, $\bar{\bar{\sigma}}$, and the depolarization ratios of the grains, $\bar{\bar{L}}$, are second rank tensors, and the relationship between them is very complicated. If the composite medium is macroscopically isotropic, corresponding to random orientations of insulating spheroids, $\bar{\bar{\sigma}}$ is a scalar and is simply given[20,21] by

$$\sigma=\sigma_f P^m \ , \tag{B11}$$

where σ_f is the fluid conductivity, P is the porosity, and m is given by

$$m=\frac{1}{3}\left\langle\frac{1}{1-L_x}+\frac{1}{1-L_y}+\frac{1}{1-L_z}\right\rangle \quad . \tag{B12}$$

Here the angular brackets denote average over the ellipticities where the subscripts in (B12) now refer to principal axes of the ellipsoid and not to the field direction. Using the fact that $L_y=L_z=\frac{1}{2}(1-L_s)$, for spheroids whose x axis is the symmetry axis $L_x=L_s$, (B12) gives

$$m=\frac{1}{3}\left\langle\frac{5-3L_s}{1-L_s^2}\right\rangle$$

or

$$m=\tfrac{1}{3}\int\frac{5-3L_s}{1-L_s^2}P(L_s)\,dL_s \quad , \tag{B13}$$

where $P(L_s)$ is the probability distribution of depolarization factor L_s. For a sample consisting of spherical grains only, the distribution is $P(L_s)=\delta(L_s-\frac{1}{3})$ (because $L_s=L_y=L_z=\frac{1}{3}$), and therefore we have

$$m(\text{spheres})=\tfrac{3}{2} \quad . \tag{B14}$$

For a sample consisting of a random array of randomly oriented needles, we have $P(L_s)=\delta(L_s)$ from (B6) and therefore

$$m(\text{random needles})=\tfrac{5}{3} \quad . \tag{B15}$$

Next, consider the anisotropic materials. If all the grains are ellipsoids of the same shape but arbitrary size and oriented with all their principal axes in the same directions, taken to be the coordinate axes, then the conductivity tensor and the depolarization tensor are diagonal. The diagonal elements of the conductivity, σ_{xx} for example, are related to the depolarization factors via a transcendental equation (A12), of Mendelson and Cohen.[21] This is because an ellipsoid embedded in an anisotropic effective medium produces a nonuniform field outside the ellipsoid which mixes the field components in the different directions and thus the conductivities in the different directions; in integrating to the final concentration of grains in the self-similar model, the effective host medium at each stage is, of course, anisotropic even though the pore fluid itself is isotropic. There is no problem for the isotropic host effective medium corresponding to a random orientation of grains.

For the cases of extreme ellipticity, however, we can still obtain simple expressions for the conductivity. For aligned needles or tubes (prolate spheroids with eccentricity $e\equiv 1$) embedded in a conducting fluid the conductivity along the direction of the symmetry axes is *exactly* given by

$$\sigma(\text{needles, parallel})\equiv\sigma_f P \quad . \tag{B16}$$

The conductivity in a direction perpendicular to the symmetry axes is obtained directly from Eq. (A12) of Mendelson and Cohen[21] within the self-similar model and (B16) (above):

$$\sigma(\text{needles, perpendicular})=\sigma_f P^2 \quad . \tag{B17}$$

For aligned plates (oblate spheroids with eccentricity $e\rightarrow\infty$) embedded in a conducting fluid the exact result for conductivity parallel to the plates is

$$\sigma(\text{plates, parallel})\equiv\sigma_f P \quad , \tag{B18}$$

whereas there is no conductivity in a direction perpendicular to the plates:

$$\sigma(\text{plates, perpendicular})\equiv 0 \quad . \tag{B19}$$

Equations (B16)–(B19) are also of the form of Eq. (B11) or equivalently (4.4),

$$\sigma_{ii}=\sigma_f P^m \tag{B20}$$

for conductivity along the ith direction and the exponent is related to the pertinent depolarization factor by

$$m=\frac{1}{1-L_i} \tag{B21}$$

as can easily be checked from (B6) and (B7).

The self-similar model for the conductivity is of the form of Eq. (B11) and (B13) for random orientations of spheroids of arbitrary eccentricity. For aligned spheroids, the conductivity tensor of the anisotropic macroscopic medium is given by Eqs. (B20) and (B21) for spheres ($L_i=\frac{1}{3}$, $m=\frac{3}{2}$), plates, or needles; we surmise that Eqs. (B20) and (B21) are reasonable approximations to the full self-similar model for aligned spheroids of arbitrary eccentricity.

The procedure used by Veinberg[21] (and its application to rocks by Mendelson and Cohen[21]) did not employ the coated ellipsoid technique. Veinberg[21] introduces grains by an infinitesimal amount at each step into the previous mixture and uses the effective-medium approximation (EMA) at each step. Since only an infinitesimal amount of grain is introduced at each step (far below the precolation threshold), the medium remains conducting at each step. Furthermore, for coated spheres, EMA is equivalent to uncoated spheres with the Clausius-Mossotti [average T-matrix approximation (ATA)].[20] But, ATA in turn is the same as EMA in the dilute concentration limit.[20] Thus the procedures in Refs. 19 and 20 are equivalent for spheres. Although we have not proved this in detail for nonspherical cases (other than needles and plates) we expect that using coated ellipsoid, is equivalent to using uncoated ones, provided that we use the correct boundary contition, i.e., start with fluid at step zero.

[1]Lord Rayleigh (J. W. Strutt), *Theory of Sound,* 2nd ed. (MacMillan, London, 1878) (Dover, New York, 1945).
[2]I. Rudnick, in *New Directions in Physical Acoustics, Proceedings of the International School of Physics "Enrico Fermi," Course LXIII,* edited by D. Sette (North-Holland, Elsevier, New York, 1976), p. 112.
[3]L. D. Landau and E. M. Lifshitz, *Fluid Mechanics* (Pergamon, New York, 1959).
[4]Ref. 3, p. 24.
[5]Ref. 3, p. 11ff.
[6]R. J. S. Brown, Geophysics 45, 1269 (1980).
[7]D. J. Bergman, B. I. Halperin, and P. C. Hohenberg, Phys. Rev. B 11, 4253 (1975).
[8]D. J. Bergman, J. Phys. C 12, 4947 (1979).
[9]Lord Rayleigh (J. W. Strutt), Philos. Mag. 34, 481 (1892).
[10]J. C. Maxwell, *A Treatise on Electricity and Magnetism* (Dover, New York, 1954) (orig. ed. 1873).
[11]M. H. Cohen, Geophysics 46, 1057 (1981).
[12]D. L. Johnson, Appl. Phys. Lett. 37, 1065 (1980).
[13]M. A. Biot, J. Acoust. Soc. 28, 168 (1956); 28, 179(1956); 34, 1254 (1962); J. Appl. Phys. 33, 1482 (1962); M. A. Biot and D. G. Willis, J. Appl. Mech. 24, 594 (1957).
[14]T. J. Plona and D. L. Johnson (unpublished).
[15]D. L. Johnson (unpublished).
[16]M. Revzen, B. Shapiro, C. G. Kuper, and J. Rudnick, Phys. Rev. Lett. 33, 143 (1974).
[17]H. Kojima, W. Veith, S. J. Putterman, E. Guyon, and I. Rudnick, Phys. Rev. Lett. 27, 714 (1971); H. Kojima, W. Veith, E. Guyon, and I. Rudnick, J. Low Temp. Phys. 25, 195 (1976).
[18]J. B. Mehl and W. Zimmerman, Phys. Rev. 167, 214 (1968).
[19]H. Fricke, Phys. Rev. 24, 575 (1924).
[20]P. N. Sen, C. Scala, and M. H. Cohen, Geophysics 46, 781 (1981).
[21]K. Mendelson and M. H. Cohen, Geophysics (in press); A. K. Veinberg, Sov. Phys. Dokl. 11, 593 (1967) [Dok. Akad. Nauk SSSR 169, 543 (1966)].
[22]K. A. Shapiro and I. Rudnick, Phys. Rev. 137, A1383 (1965).
[23]M. Kriss and I. Rudnick, J. Low Temp. Phys. 3, 339 (1970).
[24]J. M. Ziman, *Models of Disorder* (Cambridge University, Cambridge, England, 1979).
[25]W. McCrone, J. A. Brown, and I. M. Stewart, *Particle Atlas* (Ann Arbor Science, Ann Arbor, 1980), Vol. VI.
[26]R. Rosenbaum, G. A. Williams, D. Heckerman, J. Marcus, D. Schaller, J. Maynard, and I. Rudnick, J. Low Temp. Phys. 37, 663 (1979).
[27]R. Kleinberg (private communication).
[28]K. Kendall, Contemp Phys. 21, 277 (1980).
[29]H. Kojima, D. N. Paulson, and J. C. Wheatley, Phys. Rev. Lett. 32, 141 (1974); J. Low Temp. Phys. 21, 283 (1975).
[30]M. A. Ferrero and G. G. Sacerdote, Acoustic 1, 137 (1951).
[31]L. D. Landau and E. M Lifshitz, *Electrodynamics of Continuous Media* (Pergamon, New York, 1960).
[32]J. A. Stratton, *Electromagnetic Theory* (McGraw-Hill, New York, 1941).